International Tables for Crystallography (2006). Vol. C, Chapter 4.1, pp. 186–190.

4.1. Radiations used in crystallography

By V. Valvoda

4.1.1. Introduction

The radiations used in crystallography are either electromagnetic waves or beams of particles. The choice of radiation depends on the type of crystallographic information needed. The most general tool for obtaining any crystallographic information is diffraction but other types of scattering or reflection and absorption phenomena are also used in *general* crystallography (see Fig. 4.1.1.1).

4.1.2. Electromagnetic waves and particles

Both electromagnetic waves and particles can be described by the wavefunction $\psi(\mathbf{r})$, as a complex function of spatial coordinates, by the wavelength λ, the wavevector $\mathbf{k}$, which indicates the direction of propagation and is of magnitude $2\pi/\lambda$, the frequency ν or angular frequency ω in rad s^{-1}, and the phase velocity v (and the group velocity). Intensity in $\mathbf{r}$ is given by $|\psi(\mathbf{r})|^2$. These wavefunctions are solutions of the same type of differential equation [see, for example, Cowley (1975)]:

$$\nabla^2\psi + k^2\psi = 0. \tag{4.1.2.1}$$

For electromagnetic waves,

$$k^2 = \varepsilon\mu\omega^2 = \omega^2/v^2, \tag{4.1.2.2}$$

where k is the wavenumber, ε is the permittivity or dielectric constant and μ is the magnetic permeability of the medium; $\mu \approx 1$ for most cases. The velocity of the waves in free space is $c = 1/(\varepsilon_0\mu_0)^{1/2}$; otherwise $v = c/n$, where $n = (\varepsilon/\varepsilon_0)^{1/2}$ is the refraction index.

For particles of mass m and charge q with kinetic energy E_k in field-free space, the wave equation (4.1.2.1) is the time-independent Schrödinger equation and

$$k^2 = \frac{8\pi^2 m}{h^2}\{E_k + q\mathscr{S}(\mathbf{r})\}, \tag{4.1.2.3}$$

where $\mathscr{S}(\mathbf{r})$ is the electrostatic potential function and the bracket gives the sum of the kinetic and potential energies of the particles.

Important nontrivial solutions of (4.1.2.1) are (after adding the time dependence) the plane wavefunctions

$$\psi = \psi_0 \exp\{i(\omega t - \mathbf{k}\cdot\mathbf{r})\} \tag{4.1.2.4}$$

or the spherical wavefunctions

$$\psi = \psi_0 \frac{\exp\{i(\omega t - kr)\}}{r}. \tag{4.1.2.5}$$

Thus, relatively simple semi-classical wave mechanics, rather than full quantum mechanics, is needed for interactions with no appreciable loss of energy. The interaction of the waves with matter depends on the spatial variation of the refractive index given by the spatial variations of the electron density or the electrostatic potential functions.

Electromagnetic waves can also be described in terms of energy quanta, photons, with energy given by Planck's law

$$E = h\nu. \tag{4.1.2.6}$$

The values of E, ν, and λ of the electromagnetic waves used in general crystallography are scaled in Fig. 4.1.2.1. It should be noted that there are several types of electromagnetic waves in the most important wavelength range near 1 Å, which are called X-rays (when generated in X-ray tubes), γ-rays (when emitted by radioactive isotopes) or synchrotron radiation (emitted by electrons moving in a circular orbit).

On the other hand, the beam of particles of mass m, moving with velocity v, behaves like waves with wavelength given by de Broglie's law

$$\lambda = \frac{h}{mv} \tag{4.1.2.7}$$

or using $E_k = \frac{1}{2}mv^2$ for the kinetic energy of particles

$$\lambda = \frac{h}{(2mE_k)^{1/2}}. \tag{4.1.2.8}$$

When relativistic effects are taken into account,

$$\lambda = \lambda_0\left\{1 + \frac{E_k}{2m_0c^2}\right\}^{-1/2}, \tag{4.1.2.9}$$

where m_0 is the rest mass and λ_0 the non-relativistic wavelength. High-energy electrons ($E_k \approx 10^5$ eV, $\lambda \approx 10^{-2}$ Å) and neutrons ($E_k \approx 10^{-2}$ eV, $\lambda \approx 10^0$ Å) belong to the most prominent particles used in diffraction crystallography (see Table 4.1.3.1). However, low-energy electrons ($E_k \approx 10^2$ eV,

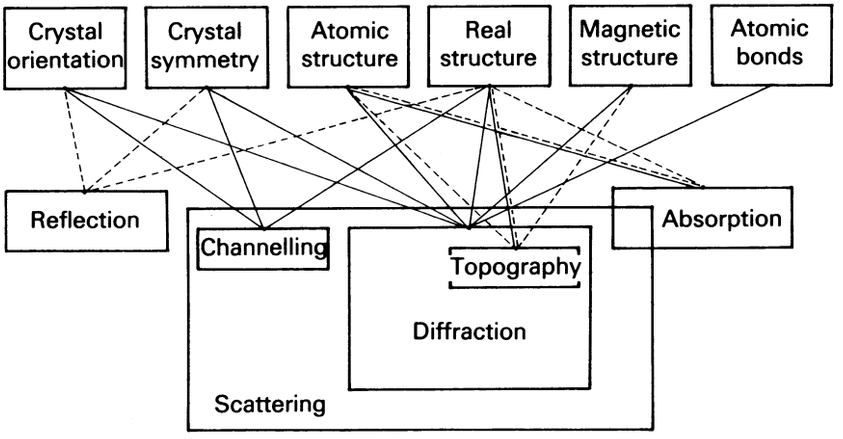

Fig. 4.1.1.1. Schematic diagram of the main types of radiation application in crystallography (dashed lines represent structure investigation on a larger than atomic scale).

$\lambda \approx 10^0$ Å), protons or ions of elements with quite high atomic number and energy ($E_k \approx 10^3 - 10^6$ eV) are also used in scattering, channelling or shadowing experiments (see Section 4.1.5).

4.1.3. Most frequently used radiations

Average diffraction properties of X-rays, high-energy electrons, and neutrons are listed in Table 4.1.3.1. They can be varied with respect to the material analysed by changing the incident-beam operating conditions and they also greatly depend on the mutal interaction of radiation with the material. The values presented are typical rather than extreme ones and should be used as a guide for rough estimates and for general orientation in the subject. Details are given in the following sections. The properties of the radiations and the features of their interaction with crystals also impose limitations on the sample choice or preparation, on the recording of the diffraction data, and on the theoretical interpretation of these data. The different nature of the scattering of X-rays and electrons (interacting with the electron-density distribution or with the potential distribution) and neutrons (which are mainly scattered by nuclei) may be used in combined experiments to study details of thermal smearing of atomic positions and bonding characteristics of the electron-density distribution.

Table 4.1.3.1. *Average diffraction properties of X-rays, electrons, and neutrons*

	X-rays	Electrons	Neutrons
(1) Charge	0	-1 e	0
(2) Rest mass	0	9.11×10^{-31} kg	1.67×10^{-27} kg
(3) Energy	10 keV	100 keV	0.03 eV
(4) Wavelength	1.5 Å	0.04 Å	1.2 Å
(5) Bragg angles	Large	1°	Large
(6) Extinction length	10 μm	0.03 μm	100 μm
(7) Absorption length	100 μm	1 μm	5 cm
(8) Width of rocking curve	5"	0.6°	0.5"
(9) Refractive index	$n < 1$	$n > 1$	$n \lesssim 1$
$n = 1 + \delta$	$\delta \approx -1 \times 10^{-5}$	$\delta \approx +1 \times 10^{-4}$	$\delta \approx \mp 1 \times 10^{-6}$
(10) Atomic scattering amplitudes f	10^{-3} Å	10 Å	10^{-4} Å
(11) Dependence of f on the atomic number Z	$\sim Z$	$\sim Z^{2/3}$	Nonmonotonic
(12) Anomalous dispersion	Common	–	Rare
(13) Spectral breadth	1 eV $\Delta\lambda/\lambda \approx 10^{-4}$	3 eV $\Delta\lambda/\lambda \approx 10^{-5}$	500 eV $\Delta\lambda/\lambda \approx 2$

Notes to Table 4.1.3.1

(1) *Charge*. Charged electrons interact strongly with matter and must be used in vacuum whereas X-rays and neutrons can be used in air.

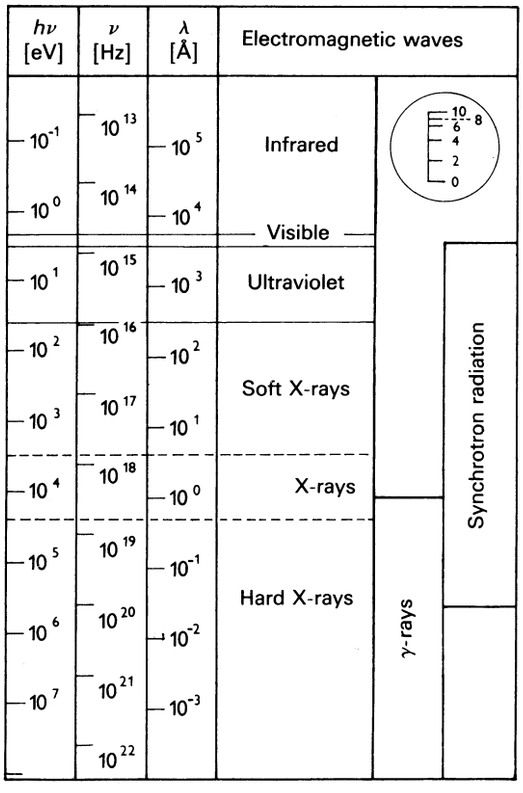

Fig. 4.1.2.1. Comparison of the energy, frequency, and wavelength of the electromagnetic waves used in crystallography (logarithmic scale).

(2) *Rest mass*. The wavelength of moving particles with the same energy is inversely proportional to the square root of their mass.

(3) *Energy*: Energies of X-rays generated in commonly used X-ray tubes range from 5 to 17 keV. High-energy electrons used in electron microscopes have energies from 40 to 300 keV, but energies of 1 MeV or more are achievable (for low-energy electrons, see Subsection 4.1.4.2). The extremely low energy of neutrons as compared with X-rays or electrons leads to their strong inelastic interaction with phonons (see Subsection 4.1.4.3).

(4) *Wavelength*. The radius of the Ewald sphere for electrons is much larger than that for X-rays or neutrons and thus part of the reciprocal-lattice plane image can be seen immediately if fixed-crystal electron diffraction is used. Wavelengths of electrons and neutrons are tunable by changing instrumental conditions (high voltage in the microscope and the temperature inside the reactor, respectively) whereas X-ray wavelengths are given by discrete lines of the characteristic spectra of the X-ray tube targets (for other X-ray sources, see Subsection 4.1.4.1).

(5) *Bragg angles*. The whole observable diffraction pattern obtained by electrons is contracted into small angles not exceeding 3–5° with the primary beam.

(6) *Extinction length*. The extinction length corresponds to the thickness of the crystal required for the whole incident beam to be scattered into the Bragg reflected beam and then to be scattered back into the direction of the incident beam. If the size of a nearly perfect crystal (or the size of the mosaic blocks) is comparable to or exceeds the extinction length for the given reflection then the dynamic diffraction theory (or the primary-extinction correction of applied kinematic theory in

the case of the mosaic crystal) must be used. The dynamical effects thus decrease when passing from electrons to X-rays and neutrons for a given crystal thickness.

(7) *Absorption length*. Absorption length is here estimated by the reciprocal values of the linear absorption coefficients. The value of the absorption length determines the size of the sample or the surface layer thickness accessible for diffraction analysis. The penetration of the electron beam into the crystal is severely limited by absorption or by diffraction when a strong reflection is excited and thus only 10–1000 Å surface layers contribute to the electron diffraction. Owing to the Borrmann effect, there occurs a substantial decrease of X-ray absorption for nearly perfect crystals in diffraction position. The relatively large crystals used for neutron diffraction in order to obtain useful diffraction intensities have been found to cause particularly important secondary-extinction effects due to disorientation of the mosaic blocks.

(8) *Width of rocking curve*. The range of angles between a crystal plane and the diffracted beam over which there is significant Bragg reflection is much larger for electrons than for X-rays or neutrons.

(9) *Refractive index*. The refractive index deviates slightly from unity for the radiations compared and the angle of refraction thus makes only a few angular minutes and increases with increasing wavelength. Negative values of δ for neutrons correspond to positive values of atomic scattering amplitudes and *vice versa*. The refraction effects will be considerable for the small angles of incidence of electrons needed in the Bragg case of diffraction (see *Bragg angles*) and the waves diffracted from planes parallel to the surface having spacings as small as 2 or 3 Å may suffer total internal reflection and be unable to leave the crystal.

(10) *Atomic scattering amplitudes*. The example given corresponds to the scattering of the atoms of lead at $(\sin\theta)/\lambda = 0.4\,\text{Å}^{-1}$. The absolute values of the atomic scattering amplitudes for electrons are considerably greater than for X-rays or neutrons; this is also reflected in the structure-amplitude values and in the corresponding intensities of the Bragg reflections. For the angular dependence of the atomic scattering amplitudes, see Fig. 4.1.3.1. The constant value of the atomic scattering amplitudes for neutrons (also often called the scattering length) makes neutron diffraction suitable for precise measurement of thermal parameters.

(11) *Dependence of atomic scattering amplitudes on the atomic number Z*. This kind of dependence is illustrated for neutral atoms in Fig. 4.1.3.2. Because of the relatively weaker dependence on the atomic number, the peaks of light atoms in the presence of heavy atoms are revealed more clearly in the Fourier synthesis of electron-density maps obtained by the electron-diffraction method than by X-ray diffraction. The same is generally true for neutron diffraction, which also enables atoms of elements with similar atomic numbers to be distinguished in certain cases (based on the irregular change of atomic scattering amplitudes with Z); different isotopes of the same element may also be distinguished.

(12) *Anomalous dispersion*. This effect is utilized for the solution of the phase problem in crystal structure analysis by X-ray diffraction. In the case of neutron diffraction, there are only a few stable isotopes convenient for this purpose (mainly ^{149}Sm, ^{157}Gd, and ^{113}Cd). The wavelength of the high-energy electrons is too short compared with the K-absorption edges of atoms and the resonance scattering of electrons is thus negligible.

(13) *Spectral breadth*. The value for X-rays corresponds to the characteristic lines of X-ray spectra. The spread of energies or wavelengths in the beam of neutrons obtained from a reactor is quite broad and for diffraction experiments a narrow range of wavelengths is usually selected by the use of a crystal monochromator or, especially for long wavelengths, by a time-of-flight chopper device that selects a range of neutron velocities.

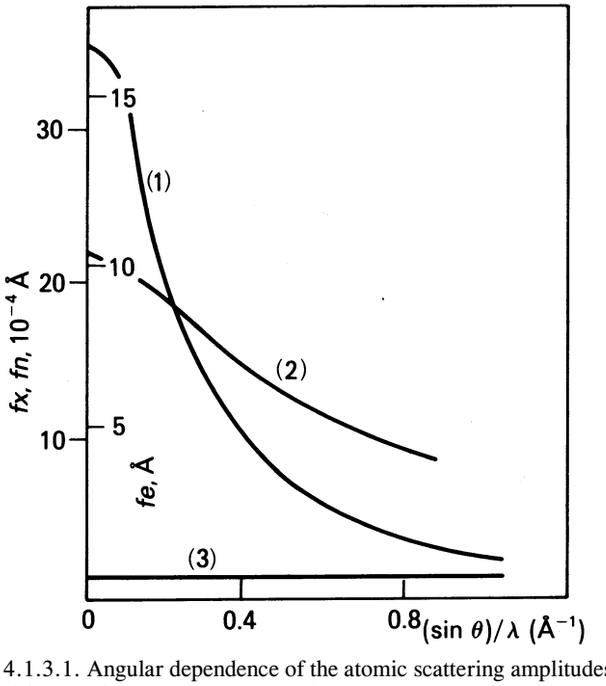

Fig. 4.1.3.1. Angular dependence of the atomic scattering amplitudes of lead for (1) electron, (2) X-ray, and (3) neutron scattering (in absolute values).

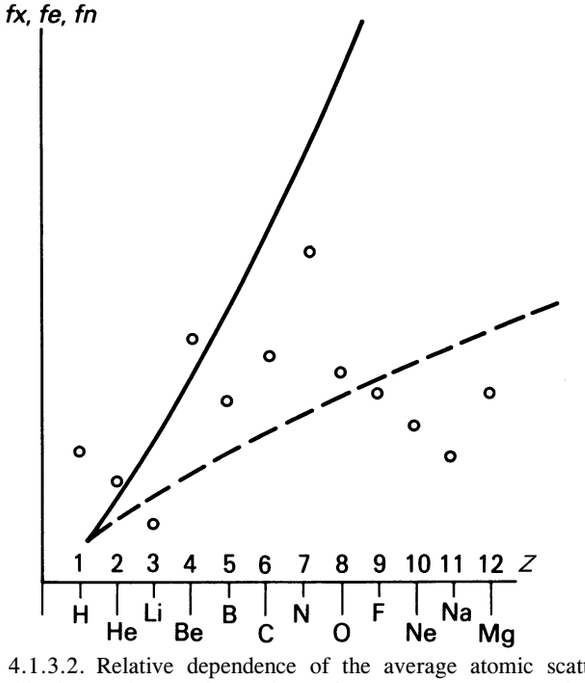

Fig. 4.1.3.2. Relative dependence of the average atomic scattering amplitudes on the atomic number Z for X-rays (———), electrons (— — —), and neutrons (○). The values plotted are averages over $(\sin\theta)/\lambda$.

4.1.4. Special applications of X-rays, electrons, and neutrons

Special sources and/or special properties of these radiations are used in general crystallography.

4.1.4.1. *X-rays, synchrotron radiation, and γ-rays*

X-ray beams from *rotating-anode tubes* are approximately one hundred times more intensive than those from normal X-ray tubes. *Laser plasma X-ray sources* yield intensive nanosecond pulses of the line spectrum of nearly electron-free ions in the X-ray region with a spectral breadth of $\Delta\lambda/\lambda \approx 10^{-3}$. Several such pulses may be repeated per hour (Frankel & Forsyth, 1979). *Synchrotron radiation* is characterized by a continuous spectrum of wavelengths, high spectral flux, high intensity, high brightness, extreme collimation, sharp time structure (pulses with 30–200 ps length emitted in ns intervals), and nearly 100% polarization in the orbital plane (Kuntz, 1979; Bonse, 1980). Some of these properties are utilized in ordinary structure analysis: for example, fine tuning of the wavelength of synchrotron radiation for the solution of the phase problem by resonant scattering on chosen atomic species constituting the material under study. But these radiations also offer new advantages in other fields of crystallography, as, for example, in X-ray topography (Tanner & Bowen, 1980), in time-resolving studies (Bordas, 1980), in X-ray microscopy (Parsons, 1980), in studies of local atomic arrangements by extended X-ray absorption fine structure (XAFS) investigations (Lee, Citrin, Eisenberger & Kincaid, 1981) or studies of surface structures by X-ray photoemission spectroscopy (XPS) (Plummer & Eberhardt, 1982), *etc*. *γ-rays* emitted by radioactive sources such as ^{198}Au ($t_{1/2} = 2.7$ d), ^{153}Sm ($t_{1/2} = 46.8$ h), ^{192}Ir ($t_{1/2} = 74.2$ d) or ^{137}Cs ($t_{1/2} = 29.9$ a) are characterized by short wavelengths (typically hundreds of Å), by narrow spectral breadth ($\Delta E \approx 10^{-8}$ eV, $\Delta\lambda/\lambda \approx 10^{-6}$) and by relatively low beam intensity ($\sim 10^8 - 10^9$ m^{-2} s^{-1}). They are mainly used for studies of the mosaic structure of single crystals (Schneider, 1983) or for the determination of charge density distribution (Hansen & Schneider, 1984). The typical absorption length of $\sim$ 1–4 cm and the increase of the extinction length by a factor of about 50 compared with ordinary X-rays are advantages utilized in these experiments. γ-rays also find applications in magnetic structure studies and in the determination of gradients of electric fields by Mössbauer diffraction and spectroscopy (Kuz'min, Kolpakov & Zhdanov, 1966).

For Compton scattering, see Sections 6.1.1 and 7.4.3.

4.1.4.2. *Electrons*

Low-energy electrons (10–200 eV) have wavelengths near 1 Å and a penetration of a few Å below the surface of a crystal. Low-energy electron diffraction (LEED) is thus used for the study of surface-layer structures (Ertl & Küppers, 1974). High-energy electrons are also currently used in electron microscopy in materials science. Under certain conditions, images of lattice planes with a resolution of 2 Å or better can be obtained. Transmission electron microscopy is also used for reconstruction of the three-dimensional structure of biological objects (such as viruses), alternatively in combination with X-ray diffraction (de Rossier & Klug, 1968).

4.1.4.3. *Neutrons*

The most important application of neutron diffraction is found in studies of magnetic structures (Marshall & Lovesey, 1971). The magnetic moment of neutrons is equal to $1.913\,\mu_N$, where μ_N is the nuclear magneton, and neutrons have spin $I = 1/2$. They can thus interact with the magnetic moments of nuclei or with the magnetic moments of the electron shells with uncompensated spins. Changes in wavelength from 1 to 30 Å enable one to study non-uniformities of different sizes and structures of polymers and biological objects by the small-angle method. Inelastic scattering of neutrons is used for determining phonon-dispersion curves. Neutron topography and neutron texture diffraction can be utilized for the relatively large samples used in technological applications. The *pulsed spallation neutron sources* are used for high-resolution time-of-flight powder diffraction (Windsor, 1981) or for time-resolved Laue diffraction.

4.1.5. Other radiations

4.1.5.1. *Atomic and molecular beams*

Fast charged particles like protons, deuterons or He^+ ions show preferential penetration through crystals when the direction of incidence is almost parallel to the prominent planes or axes of the lattice. The reverse effect of this *channelling* is *shadowing* when the centres of emission of the fast charged particles are the atoms of the crystal themselves. These methods are, for example, used in studies of surface structures, lattice defects, orientation, thermal vibrations, atomic displacements, and concentration profiles (Feldman, Mayer & Picraux, 1982). Ion beams are also applied in special analytical methods like Rutherford backscattering (RBS), inelastic scattering, proton-induced X-ray analysis (PIX), *etc*.

4.1.5.2. *Positrons and muons*

These elementary particles are used in crystallography mainly in studies of lattice defects (vacancies, interstitials, and impurity atoms) for the determination of their concentration, location, and diffusion by means of the techniques such as positron annihilation spectroscopy (PAS) and muon spin resonance (μSR) – see, for example, Siegel (1980) and Gyax, Kündig & Meier (1979). The positron implantation range in a solid is $\lesssim 100\,\mu$m from the positron sources usually used (*e.g.* ^{22}Na, ^{64}Cu, ^{58}Co); these sources yield positrons with end-point energies of $\lesssim$1 MeV. The PAS techniques are based on lifetime, Doppler broadening or angular correlation measurements of γ-rays emitted by the decaying nucleus of the radioactive source and those resulting from the positron–electron annihilation process. Muon sources require intense primary medium-energy proton beams. The positive muon μ^+ has charge +e, spin 1/2, mass $105.659\,\text{MeV}/c^2$ and a magnetic moment equal to 1.001 of the muon–magneton units. With a mean lifetime of 2.197 μs, the muon decays into a positron (e^+) and two neutrinos (ν_e and $\bar{\nu}_\mu$). The correlation between the direction of the emitted positron and the spin direction of the muon allows one to measure the spin precession frequency and/or the decay of the muon polarization of an ensemble of muons implanted in a solid.

4.1.5.3. *Infrared, visible, and ultraviolet light*

Visible light is one of the oldest tools used by crystallographers for macroscopic symmetry determination, for orientation of crystals, and in metallographic microscopes for phase analysis. Infrared and Raman spectroscopy are highly complementary methods in the infrared and visible range of wavelengths, respectively. The information content available with the two techniques is determined by molecular symmetry and polarity. This information is utilized for the identification of molecules or structural groups [symmetric

vibrations and nonpolar groups are most easily studied by Raman scattering, antisymmetric vibrations and polar groups by infrared scattering (Grasselli, Snavely & Bulkin, 1980)]. The valence states or the bonds of surface atoms and the local structure in the immediate neighbourhood of the chosen atoms can be studied by ultraviolet radiation in the energy range 10–50 eV by means of angle-resolved photoelectron emission (Plummer & Eberhardt, 1982).

4.1.5.4. *Radiofrequency and microwaves*

Electromagnetic waves of frequencies 10^6–10^{10} Hz are used in nuclear magnetic resonance (NMR) and electron paramagnetic resonance (EPR) experiments for studies of interatomic bonds, local atomic configurations, ordering, and relative population of atomic sites as well as for the determination of orientational features of magnetic structures (Kaufman & Shenoy, 1981).

References

4.1

Bonse, U. (1980). *X-ray sources. Characterization of crystal growth defects by X-ray methods*, edited by B. K. Tanner & D. K. Bowen, Chap. 11, pp. 298–319. New York: Plenum. [NATO Advanced Study Institute Series B63.]

Bordas, J. (1980). *A synchrotron radiation camera and data acquisition system for time resolved X-ray scattering studies. J. Phys. E*, **13**, 938–944.

Cowley, J. M. (1975). *Diffraction physics*, Chap. 1. Amsterdam: North-Holland.

Ertl, G. & Küppers, J. (1974). *Monographs in modern chemistry*, Vol. 4. *Energy electrons and surface chemistry*, edited by H. F. Ebel, Chap. 9, pp. 129–192. Weinheim: Verlag Chemie.

Feldman, C., Mayer, J. W. & Picraux, S. T. (1982). *Materials analysis by ion channeling*. London: Academic Press.

Frankel, R. D. & Forsyth, J. M. (1979). *Nanosecond X-ray diffraction from biological samples with a laser-produced plasma source. Science*, **204**, 622–624.

Grasselli, J. G., Snavely, M. K. & Bulkin, B. J. (1980). *Applications of Raman spectroscopy. Physics reports* 65, No. 4, pp. 231–344. Amsterdam: North-Holland.

Gyax, F. N., Kündig, W. & Meier, P. F. (1979). Editors. *Muon spin rotation*. Amsterdam: North-Holland.

Hansen, N. K. & Schneider, J. R. (1984). *Charge-density distribution of Be metal studied by γ-ray diffractometry. Phys. Rev. B*, **29**, 917–926.

Kaufmann, E. N. & Shenoy, G. K. (1981). Editors. *MRS symposia proceedings*, Vol. 3. *Nuclear and electron resonance spectroscopies applied to materials science*. New York: North-Holland.

Kunz, C. (1979). Editor. *Topics in current physics*, Vol. 10. *Synchrotron radiation, techniques and applications*. Berlin: Springer Verlag.

Kuz'min, R. N., Kolpakov, A. V. & Zhdanov, G. S. (1966). *Rassejanie messbauerovskovo izlutschenija kristallami. Kristallografiya*, **11**, 511–519. [English translation: *Sov. Phys. Crystallogr.* (1967), **11**, 457–465.]

Lee, P. A., Citrin, P. H., Eisenberger, P. & Kincaid, B. M. (1981). *Extended X-ray absorption fine structure – its strengths and limitations as a structural tool. Rev. Mod. Phys.* **53**, 769–806.

Marshall, W. & Lovesey, S. W. (1971). *Theory of thermal neutron scattering*. Oxford: Clarendon Press.

Parsons, D. F. (1980). Editor. *Ultrasoft X-ray microscopy: its application to biological and physical sciences*. New York: New York Academy of Sciences.

Plummer, E. W. & Eberhardt, W. (1982). *Advances in chemical physics*, Vol. XLIX. *Angle-resolved photoemission as a tool for the study of surfaces*, edited by I. Prigogine & S. I. Rice. New York: John Wiley.

Rosier, D. J. de & Klug, A. (1968). *Reconstruction of three dimensional structures from electron micrographs. Nature (London)*, **217**, 130–134.

Schneider, J. R. (1983). *Characterization of crystals by γ-ray and neutron diffraction methods. J. Cryst. Growth*, **65**, 660–671.

Siegel, R. W. (1980). *Positron annihilation spectroscopy. Annu. Rev. Mater. Sci.* **10**, 393–425.

Tanner, B. K. & Bowen, D. K. (1980). Editors. *Characterization of crystal growth defects by X-ray methods*. NATO Advanced Study Institute Series B63. New York: Plenum.

Windsor, C. G. (1981). *Pulsed neutron scattering*. London: Taylor and Francis.

4.2.1

Bailey, R. L. (1978). *The design and operation of magnetic liquid shaft seals*. In *Thermomechanics of magnetic fluids*, edited by B. Berkovsky. London: Hemisphere.

Buras, B. (1985). *The European Synchrotron Radiation Project. Nucl. Sci. Appl.* **2**, 127–143.

Buras, B. & Marr, G. V. (1979). Editors. *European Synchrotron Radiation Facility*. Suppl. III: *Instrumentation*. Strasbourg: ESF.

Buras, B. & Tazzari, S. (1984). Editors. *European Synchrotron Radiation Facility*. Geneva: ESRP c/o CERN.

Byer, R. L., Kuhn, K., Reed, M. & Trail, J. (1983). *Progress in high peak and average power lasers for soft X-ray production. Proc. SPIE*, **448**, 2–7.

Castaing, R. & Descamps, J. (1955). *Sur les bases physiques de l'analyse ponctuelle par spectrographie X. J. Phys. Radium*, **16**, 304–317.

Clay, R. E. (1934). *A 5 kW X-ray generator with a spinning target. Proc. Phys. Soc. London*, **46**, 703–712.

Cohen, E. R. & Taylor, B. N. (1987). *The 1986 adjustment of the fundamental physical constants. Rev. Mod. Phys.* **89**, 1121–1148.

Collins, C. B., Davanloo, F. & Bowen, T. S. (1986). *Flash X-ray source of intense nanosecond pulses produced at high repetition rates. Rev. Sci. Instrum.* **57**, 863–865.

Compton, A. H. & Allison, S. K. (1935). *X-rays in theory and experiment*. New York: Van Nostrand.

Cosslett, V. E. & Nixon, W. C. (1951). *X-ray shadow microscope. Nature (London)*, **168**, 24–25.

Cosslett, V. E. & Nixon, W. C. (1960). *X-ray microscopy*, pp. 217–222. Cambridge University Press.

Dyson, N. A. (1973). *X-rays in atomic and nuclear physics*. London: Longman.

Ehrenberg, W. & Spear, W. E. (1951). *An electrostatic focusing system and its application to a fine focus X-ray tube. Proc. Phys. Soc. London Sect. B*, **64**, 67–75.

Farge, Y. & Duke, P. J. (1979). Editors. *European Synchrotron Radiation Facility*. Suppl. 1: *The scientific case*. Strasbourg: ESF.

Fiorito, R. B., Rule, D. W., Piestrup, M. A., Li, Q., Ho, A. H. & Maruyama, X. K. (1993). *Parametric X-ray generation from moderate-energy electron beams. Nucl. Instrum. Methods*, B**79**, 758–761.

Forsyth, J. M. & Frankel, R. D. (1980). *Flash X-ray diffraction from biological specimens using a laser-produced plasma source*. Report No. 106. Laboratory for Laser Energetics, University of Rochester, USA.

Forsyth, J. M. & Frankel, R. D. (1984). *Experimental facility for nanosecond time-resolved low-angle X-ray diffraction experiments using a laser-produced plasma source. Rev. Sci. Instrum.* **55**, 1235–1242.

Fourme, R. (1992). *Sources X intenses et cristallographie biologique. Ann. Phys. (Leipzig)*, **17**, 247–255.

Frankel, R. D. & Forsyth, J. M. (1979). *Nanosecond exposure X-ray diffraction patterns from biological specimens using a laser plasma source. Science*, **204**, 622–624.